BIFURCATION ANALYSIS AND MODEL REDICTIVE THE CONTROL OF THE JEWETT-FORGER-KRONAUER MODEL FOR CIRCADIAN RHYTHMS

Lakshmi N Sridhar

Chemical Engineering Department University of Puerto Rico Mayaguez, PR 00681

ABSTRACT

The Circadian rhythm regulates several physiological processes in human beings. Hence it is important to understand its dynamics and regulate them. There are several dynamic models describing the Circadian rhythms. One of the most commonly used modes is the Jewett-Forger-Kronauer (JFK) model. Several researchers have reported the existence of limit cycles and conducted single-objective optimization studies for the Jewett-Forger-Kronauer (JFK) model that describes Circadian rhythms. In this work, a) it is shown that the limit cycles occur because of Hopf bifurcation points b) a computational strategy to eliminate the Hopf bifurcations that cause these limit cycles is provided and c) Multiobjective nonlinear model predictive control calculations are performed, for the Circadian rhythms Jewett-Forger-Kronauer (JFK) model. Bifurcation analysis was performed with MATCONT (a MATLAB software) while the Multi-objective nonlinear model predictive control was performed with the optimization language PYOMO (a Python software).

Keywords

Optimal control, bifurcation, circadian rhythm

1. INTRODUCTION

The circadian rhythm functions as a clock that regulates many physiological processes in human beings and it is important to understand the dynamics of the Circadian rhythms. Several researchers have reported the existence of limit cycles in Circadian rhythms and conducted dynamic optimization studies on models describing circadian rhythms. In this paper bifurcation analysis and Multiobjective nonlinear model predictive control calculations are performed on the Jewett-Forger-Kronauer (JFK) model for circadian rhythms.

2. BACKGROUND

Aschoff (1965) studies the Circadian rhythms in man. Jewett (1991) investigated light-induced suppression of endogenous circadian amplitude in humans. Forger et al (1999, 2002) developed models of biological clocks Leloup and Goldbeter (1998,2003) developed models for circadian rhythms in Drosophila. Doyle et al (2006) showed that the circadian rhythm is a natural, robust, multi-scale control system. Rea et al (2008) developed an approach to understanding the impact of circadian disruption on human health. Taylor et al (2008) discussed sensitivity measures for oscillating systems: application to mammalian circadian gene network. Baggs et al (2009) studied the network features of the mammalian circadian clock Mott(2003), Bagheri and co-workers (2007, 2008) Zhang and co-workers (2012, 2013, 2016) . Serkh et al (2014) Abel et al (2016), Qiao (2017), Julius et al (2017), and performed optimization and control studies of circadian dynamics. Abel et al (2019) performed nonlinear model predictive control calculations for populations of circadian oscillators. Yin et al (2019) investigated circadian entrainment in models of circadian gene regulation. Julius et al (2019) performed time-optimal entrainment control calculations for circadian rhythms using the Jewett-Forger-Kronauer (JFK) model.

3. MOTIVATION AND OBJECTIVES

The limit cycles occur because of the existence of Hopf bifurcation points. These limit cycles are undesirable as they interrupt the Circadian rhythm and hinder optimization and control tasks. Hence they should be eliminated. This is possible by the elimination of the Hopf bifurcation points. The first objective of this work is to perform a bifurcation analysis on the Circadian rhythm dynamic model, identify the various singular points, and eliminate the Hopf bifurcation point.
All optimal control tasks for problems for problems involving circadian rhythms involve single objective optimal control. In this work, Multiobjective nonlinear model predictive control(MNLMPC) calculations are performed on the Jewett-Forger-Kronauer (JFK) model for circadian rhythms and the interaction between the Bifurcation analysis and MNLMPC is investigated. The paper is organized as follows. First, the Jewett-Forger-Kronauer (JFK) model for circadian rhythms is discussed, followed by the bifurcation analysis, the MNLMPC strategy, and the interaction between the bifurcation analysis and MNLMPC.. The results and discussion are then presented followed by the conclusions.

4. THE JEWETT-FORGER-KRONAUER (JFK) MODEL FOR CIRCADIAN RHYTHMS

In the the Jewett-Forger-Kronauer (JFK) model (Julius et al (2019)), $xval1(t), xval2(t)$ represent the states of the oscillator. The signal $u(t)$ is the input to the circadian oscillator which is utilized as a bifurcation parameter and control variable. $n(t)$ is the state of the process that represents retinal photoreceptor saturation. I is the intensity of the light input that enters the receptor. The parameter values are

$$\mu = 0.13\ h^{-1}; k = 0.55h^{-1}; \alpha_0 = 0.05h^{-1}; G = 33.75; \tau_x = 24.2h$$
$$q = 1/3;\ p = 0.5\ \beta = 0.0075h^{-1}; I_0 = 9500\ lux; k_c = 0.4h$$

The value of I is 1000 Lux. The model equations are

$$\begin{aligned}
\frac{d(xval1)}{dt} &= \frac{\pi}{12}[xval2 + \mu(\frac{1}{3}xva11 + \frac{4}{3}(xva11)^3 - \frac{256}{105}(xva11)^7) + B] \\
\frac{d(xval2)}{dt} &= \frac{\pi}{12}[q(xval2)B - (\frac{24}{0.99729\tau_x})^2 xval1 - k(xval1)B] \\
\frac{d(nval)}{dt} &= 60(\alpha(1-nval) - \beta(nval)) \\
\alpha &= \alpha_0(\frac{I}{I_0})^p \\
B &= [1-0.4(xval1)][1-k_c x_c]u
\end{aligned} \tag{1}$$

5. BIFURCATION ANALYSIS

Multiple steady-states and oscillatory behavior occur in various situations. Multiple steady states occur because of t Branch and Limit bifurcation points cause multiple steady-states. Hopf bifurcation points produce oscillatory behavior. Ions and limit cycles. The MATLAB program MATCONT . (Dhooge Govearts, and Kuznetsov, 2003; Dhooge Govearts, Kuznetsov, Mestrom and Riet, 2004). is commonly used software to locate limit points, branch points, and Hopf bifurcation points. Consider an ODE system

$$\dot{x} = f(x, \beta) \qquad (2)$$

$x \in R^n$. Defining the matrix A as

$$A = \begin{bmatrix} \frac{\partial f_1}{\partial x_1} & \frac{\partial f_1}{\partial x_2} & \frac{\partial f_1}{\partial x_3} & \frac{\partial f_1}{\partial x_4} \cdots\cdots & \frac{\partial f_1}{\partial x_n} & \frac{\partial f_1}{\partial \beta} \\ \frac{\partial f_2}{\partial x_1} & \frac{\partial f_2}{\partial x_2} & \frac{\partial f_2}{\partial x_3} & \frac{\partial f_2}{\partial x_4} \cdots\cdots & \frac{\partial f_2}{\partial x_n} & \frac{\partial f_2}{\partial \beta} \\ \cdots\cdots\cdots\cdots\cdots\cdots & & & & & \\ \cdots\cdots\cdots\cdots\cdots\cdots & & & & & \\ \frac{\partial f_n}{\partial x_1} & \frac{\partial f_n}{\partial x_2} & \frac{\partial f_n}{\partial x_3} & \frac{\partial f_n}{\partial x_4} \cdots\cdots & \frac{\partial f_n}{\partial x_n} & \frac{\partial f_n}{\partial \beta} \end{bmatrix} \qquad (3)$$

β is the bifurcation parameter. The matrix A can be written in a compact form as

$$A = [B \mid \quad \partial f / \partial \beta] \qquad (4)$$

The tangent at any point x; ($v = [v_1, v_2, v_3, v_4, \ldots . v_{n+1}]$) must satisfy

$$Av = 0 \qquad (5)$$

The matrix B must be singular at both limit and branch points.. The n+1 th component of the tangent vector v_{n+1} = 0 at a limit point (LP) and for a branch point (BP) the matrix $\begin{bmatrix} A \\ v^T \end{bmatrix}$ must be singular. At a Hopf bifurcation,

$$\det(2 f_x(x, \beta) @ I_n) = 0 \qquad (6)$$

@ indicates the bialternate product while I_n is the n-square identity matrix. Hopf bifurcations cause unwanted oscillatory behavior and should be eliminated because oscillations make optimization and control tasks very difficult. More details can be found in Kuznetsov (1998; 2009) and Govaerts [2000] .

6. MULTIOBJECTIVE NONLINEAR MODEL PREDICTIVE CONTROL ALGORITHM

Flores Tlacuahuaz(2012) first proposed the Multiobjective nonlinear model predictive control method. that does not involve weighting functions, nor does it impose additional constraints on the problem unlike the weighted function or the epsilon correction method(Miettinen, 1999). For a a set of ODE

$$\frac{dx}{dt} = F(x,u)$$
$$h(x,u) \le 0 \quad x^L \le x \le x^U; \quad u^L \le u \le u^U \tag{7}$$

let $\sum_{t_{i=0}}^{t_i=t_f} p_j(t_i)$ (j=12..n); be the variables that need to be minimized/maximized simultaneously,

t_f being the final time value, and n the total number of variables that need to be optimized simultaneously. In this MNLMPC method dynamic optimization problems that independently

minimize/maximize each variable $\sum_{t_{i=0}}^{t_i=t_f} p_j(t_i)$ are solved individually. The

minimization/maximization of each $\sum_{t_{i=0}}^{t_i=t_f} p_j(t_i)$ will lead to the values p_j^*. Then the

optimization problem that will be solved is

$$\min\left(\sum_{j=1}^{n}\left(\sum_{t_{i=0}}^{t_i=t_f} p_j(t_i) - p_j^*\right)\right)^2$$
$$subject\ to\ \frac{dx}{dt} = F(x,u); \quad h(x,u) \le 0 \tag{8}$$
$$x^L \le x \le x^U; \quad u^L \le u \le u^U$$

This will provide the control values for various times. The first obtained control value is implemented and the rest are ignored. The procedure is repeated until the implemented and the

first obtained control values are the same or if the Utopia point ($\sum_{t_{i=0}}^{t_i=t_f} p_j(t_i) = p_j^*$; for all j) is

achieved. The optimization package in Python, Pyomo (Hart et al, 2017), where the differential equations are automatically converted to algebraic equations will be used. The resulting optimization problem was solved using IPOPT (Wächter And Biegler, 2006). The obtained solution is confirmed as a global solution with BARON (Tawarmalani, M. and N. V. Sahinidis 2005). To summarize the steps of the algorithm are as follows

1. Minimize/maximize $\sum_{t_{i=0}}^{t_i=t_f} p_j(t_i)$. This will lead to the value p_j^* at various time intervals t_i. The subscript *i* is the index for each time step.
2. Minimize $(\sum_{j=1}^{n}(\sum_{t_{i=0}}^{t_i=t_f} p_j(t_i) - p_j^*))^2$. This will provide the control values for various times.
3. Implement the first obtained control values and discard the remaining.
4. The steps are repeated until there is an insignificant difference between the implemented and the first obtained value of the control variables or if the Utopia point is achieved.

7. INTERACTION BETWEEN BIFURCATION AND MNLMPC

A recently published article by Sridhar(2024a) demonstrated that when MNLMPC calculations were performed on problems that exhibited Limit and Branch points the Utopia point was always obtained. This was done by incorporating the singularity condition (because of the limit and branch points) on the co-state equation for the optimal control problem. Details can be found in Sridhar(2024a).

The tanh activation function (where a control value u is replaced by) $(u \tanh u/\varepsilon)$ is commonly used in neural nets (Dubey et al 2022; Kamalov et al, 2021 and Szandała, 2020) and optimal control problems(Sridhar 2023) to eliminate spikes in the optimal control profile. The tanh factor effectively eliminates spikes that occur in control profiles. Hopf bifurcation points cause oscillatory behavior. Oscillations are similar to spikes and the results demonstrate that the tanh factor also eliminates the Hopf bifurcation by preventing the occurrence of oscillations. Sridhar (2024b) explained with several examples how the activation factor involving the tanh function successfully eliminates the limit cycle causing Hopf bifurcation points.

8. RESULTS AND DISCUSSION

The bifurcation analysis revealed the existence of a limit point and a Hopf bifurcation point at (xval1, xval2, nval, u) values of (-0.878498 -1.519704 0.992556 0.712093) and (-0.742556 -1.292880 0.992556 0.689392) respectively. This is shown in Fig. 1. Fig. 2 shows the Limit Cycle that occurs because of the Hopf Bifurcation point. For eliminating the Hopf bifurcation point, u was replaced by u(tanh (u)/7). As a result, the Hof bifurcation point is eliminated (Fig. 3) The Hopf bifurcation point in the Circadian rhythm problem is eliminated by the tanh activation factor further justifying the conclusion arrived at by Sridhar(2024b).

For the MNLMPC calculations without the tanh activation factor,($\sum_{t_{i=0}}^{t_i=t_f}(xval1(t_i)) + \sum_{t_{i=0}}^{t_i=t_f}(xval2(t_i))$) and $\sum_{t_{i=0}}^{t_i=t_f}(nval(t_i))$ are minimized individually. No activation factor was used. The objective values obtained were -7.3483513935981613 and 0.9919742.
For the multiobjecitve optimization calculations without the activation function,

$$(\sum_{t_{i=0}}^{t_i=t_f}(xval1(t_i)) + \sum_{t_{i=0}}^{t_i=t_f}(xval2(t_i)) + 7.3483513935981613)^2 + (\sum_{t_{i=0}}^{t_i=t_f}(nval(t_i)) - 0.9919742)^2$$

was minimized. The objective function value obtained was 0, implying that the Utopia point is achieved. The resulting MNLMPC control value obtained was 1.3496246229247468 . For the MNLMPC calculations with the tanh activation factor,

$(\sum_{t_{i=0}}^{t_i=t_f}(xval1(t_i))+\sum_{t_{i=0}}^{t_i=t_f}(xval2(t_i))$) and $\sum_{t_{i=0}}^{t_i=t_f}(nval(t_i))$ are minimized individually. u was

replaced by(utanh (u)/7) ,The objective values obtained were --6.9661843525677547and -1.0091977500402809.

For the multiobjecitve optimization calculations with the activation function,

$$(\sum_{t_{i=0}}^{t_i=t_f}(xval1(t_i))+\sum_{t_{i=0}}^{t_i=t_f}(xval2(t_i))+6.9661843525677547e)^2+(\sum_{t_{i=0}}^{t_i=t_f}(nval(t_i))+1.0091977500402809)^2$$

was minimized. The objective function value obtained was 0, implying that the Utopia point is achieved. The resulting MNLMPC control value obtained was 0.01531203269734607 For the Jewett-Forger- Kronauer (JFK) model describing circadian rhythms, the presence of the limit point causes the MNLMPC calculations to converge to the Utopia point validating the conclusion of Sridhar (2024a). Figures 4 and 5 show the variables and control profiles when no activation factor was used. Figures 6 and 7 show the same profiles when u was replaced but u(tanh(u))/7. A comparison of Figures 5 and 7 shows that using the activation factor eliminates the spikes in the control profile.

The bifurcation calculations are performed with MATCONT and PYOMO is used for the MNLMPC calculations following the procedures described in the earlier sections. The time period is 24 hours.

9. Conclusions and Future work

The results in this work indicate that the limit cycles in the Jewett-Forger- Kronauer (JFK) model for circadian rhythms are caused by the existence of the presence of Hopf bifurcation points which can be eliminated by the use of an activation factor involving the tanh function. This activation factor also eliminates the spikes in the control profiles when Multi objective nonlinear model predictive control calculations are performed. The Bifurcation analysis also exhibited a limit point, enabling the Multi objective nonlinear model predictive control calculations to converge to the Utopia solution. Future work will involve the performance of a combination of bifurcation analysis and Multi objective nonlinear model predictive control calculations on more advanced Circadian rhythm models.

Data Availability Statement

All data used is presented in the paper

Conflict of interest

The author, Dr. Lakshmi N Sridhar has no conflict of interest.

REFERENCES

[1] Aschoff J. Circadian rhythms in man. Science. 1965; 148(3676):1427–1432. https://doi.org/10.1126/science.148.3676.1427 PMID: 14294139

[2] Rea MS, Bierman A, Figueiro MG, Bullough JD. A new approach to understanding the impact of circadian disruption on human health. J Circadian Rhythms. 2008; 6(1):7. https://doi.org/10.1186/1740- 3391-6-7 PMID: 18510756

[3] Baggs JE, Price TS, DiTacchio L, Panda S, FitzGerald GA, Hogenesch JB. Network features of the mammalian circadian clock. PLoS Biol. 2009; 7(3):563–575. https://doi.org/10.1371/journal.pbio.1000052

[4] Leloup JC, Goldbeter A. A model for circadian rhythms in Drosophila incorporating the formation of a complex between the PER and TIM proteins. J Biol Rhythms. 1998; 13:70–87. https://doi.org/10.1177/ 074873098128999934 PMID: 9486845

[5] Leloup JC, Goldbeter A. Toward a detailed computational model for the mammalian circadian clock. Proc Nati Acad Sci USA. 2003; 100:7051–7056. https://doi.org/10.1073/pnas.1132112100

[6] Forger DB, Jewett ME, Kronauer RE. A simpler model of the human circadian pacemaker. J Biol. Rhythms. 1999; 14(6):533–538. https://doi.org/10.1177/074873099129000867

[7] Forger DB, Kronauer RE. Reconciling mathematical models of biological clocks by averaging on approximate manifolds. SIAM J Appl Math. 2002; 62:1281–1296. https://doi.org/10.1137/ S0036139900373587

[8] Doyle FJ III, Gunawan R, Bagheri N, Mirsky H, To TL. Circadian rhythm: A natural, robust, multi-scale control system. Comput Chem Eng. 2006; 30(10-12):1700–1711. https://doi.org/10.1016/j.compchemeng.2006.05.029

[9] Abel JH, Chakrabarty A, Doyle FJ III. Controlling biological time: nonlinear model predictive control for populations of circadian oscillators. In: Tempo R, Yurkovich S, Misra P, editors. Emerging Applications of Control and Systems Theory. Lecture Notes in Control and Information Sciences. Springer; 2018. p. 123–138. https://doi.org/10.1007/978-3-319-67068-3_9

[10] Mott C, Mollicone D, van Wollen M. Modifying the human circadian pacemaker using model based predictive control. In: Proc Am Control Conf. 2003; p. 453–458.

[11] Bagheri N, Stelling J, Doyle FJ III. Circadian phase entrainment via nonlinear model predictive control. Int J Robust Nonlin. 2007; 17(17):1555–1571. https://doi.org/10.1002/rnc.1209

[12] Bagheri N, Stelling J, Doyle FJ. Circadian phase resetting via single and multiple control targets. PLoS Comput Biol. 2008; 4(7):e1000104. https://doi.org/10.1371/journal.pcbi.1000104 PMID: 18795146

[13] Abel JH, Doyle FJ. A systems theoretic approach to analysis and control of mammalian circadian dynamics. Chem Eng Res Des. 2016; 116:48–60. https://doi.org/10.1016/j.cherd.2016.09.033 PMID:28496287

[14] Zhang JX, Wen JT, Julius AA. Optimal circadian rhythm control with light input for rapid entrainment and improved vigilance. In: Proc IEEE Conf Decis Control; 2012. p. 3007–3012.

[15] Zhang JX, Wen JT, Julius AA. Optimal and feedback control for light-based circadian entrainment. In: Proc IEEE Conf Decis Control; 2013. p. 2677–2682.

[16] Zhang JX, Qiao W, Wen JT, Julius AA. Light-based circadian rhythm control: Entrainment and optimization. Automatica. 2016; 68:44–55. https://doi.org/10.1016/j.automatica.2016.01.052

[17] Qiao W, Wen JT, Julius AA. Entrainment control of phase dynamics. IEEE Trans Autom Control. 2017; 62(1):445–450. https://doi.org/10.1109/TAC.2016.2555885

[18] Julius AA, Yin J, Wen JT. Time-optimal control for circadian entrainment for a model with circadian and sleep dynamics. In: Proc IEEE Conf Decis Control. Melbourne, Australia; 2017. p. 4709–4714.

[19] Serkh K, Forger DB. Optimal schedules of light exposure for rapidly correcting circadian misalignment. PLOS Comput Biol. 2014; 10(4):e1003523. https://doi.org/10.1371/journal.pcbi.1003523 PMID: 24722195 Time optimal entrainment control for circadian rhythm PLOS

[20] Taylor SR, Gunawan R, Petzold LR, Doyle FJ III. Sensitivity measures for oscillating systems: application to mammalian circadian gene network. IEEE Trans Autom Control. 2008; 53:177–188. https://doi.org/10.1109/TAC.2007.911364

[21] Jewett ME, Kronauer RE, Czeisler CA. Light-induced suppression of endogenous circadian amplitude in humans. Nature. 1991; 350:59–62. https://doi.org/10.1038/350059a0 PMID: 2002845

[22] Yin J, Julius AA, Wen JT. Rapid circadian entrainment in models of circadian genes regulation. In: ProcIEEE Conf Decis Control. 2019.
[23] Julius AA, Yin J, Wen JT (2019) Time optimal entrainment control for circadian rhythm. PLoS ONE 14(12): e0225988. https://doi.org/ 10.1371/journal.pone.0225988
[24] Sridhar. L. N. 2023 Bifurcation Analysis and Optimal Control of the Tumor Macrophage Interactions. *Biomed J Sci & Tech Res* 53(5). BJSTR. MS.ID.008470.**DOI:** 10.26717/BJSTR.2023.53.008470
[25] Sridhar LN. Coupling Bifurcation Analysis and Multiobjective Nonlinear Model Predictive Control. Austin Chem Eng. 2024a; 10(3): 1107.
[26] Sridhar LN. Elimination of oscillation causing Hopf bifurcations in engineering problems. Journal of Applied Math. 2024b; 2(4): 1826. https://doi.org/10.59400/jam1826
[27] Szandała, T. 2020, Review and Comparison of Commonly Used Activation Functions for Deep Neural Networks. *ArXiv*. https://doi.org/10.1007/978-981-15-5495-7
[28] Kamalov A. F. Nazir M. Safaraliev A. K. Cherukuri and R. Zgheib 2021, "Comparative analysis of activation functions in neural networks," *2021 28th IEEE International Conference on Electronics, Circuits, and Systems (ICECS),* Dubai, United Arab Emirates, , pp. 1-6, doi:10.1109/ICECS53924.2021.9665646.
[29] Dubey S. R. Singh, S. K. & Chaudhuri B. B. 2022 Activation functions in deep learning: A comprehensive survey and benchmark. *Neurocomputing, 503*, 92-108. https://doi.org/10.1016/j.neucom.2022.06.111
[30] Dhooge, A., Govearts, W., and Kuznetsov, A. Y., MATCONT: "A Matlab package for numerical bifurcation analysis of ODEs", *ACM transactions on Mathematical software* 29(2) pp. 141-164, 2003.
[31] Dhooge, A.,W. Govaerts; Y. A. Kuznetsov, W. Mestrom, and A. M. Riet , "CL_MATCONT"; *A continuation toolbox in Matlab,* 2004.
[32] Flores-Tlacuahuac, A. Pilar Morales and Martin Riveral Toledo; "Multiobjective Nonlinear model predictive control of a class of chemical reactors" . *I & EC research*; 5891-5899, 2012.
[33] Govaerts, w. J. F., "Numerical Methods for Bifurcations of Dynamical Equilibria", *SIAM*, 2000.
[34] Kuznetsov,Y.A. "Elements of applied bifurcation theory" .*Springer*,NY, 1998.
[35] Kuznetsov,Y.A.(2009)."Five lectures on numerical bifurcation analysis" ,*Utrecht University,N*L., 2009.
[36] Miettinen, Kaisa, M., "Nonlinear Multiobjective Optimization"; *Kluwers international series,* 1999
[37] Wächter, A., Biegler, L. "On the implementation of an interior-point filter line-search algorithm for large-scale nonlinear programming". *Math. Program.* **106**, 25–57 (2006). https://doi.org/10.1007/s10107-004-0559-y
[38] Hart, William E., Carl D. Laird, Jean-Paul Watson, David L. Woodruff, Gabriel A. Hackebeil, Bethany L. Nicholson, and John D. Siirola. "Pyomo – Optimization Modeling in Python*"* Second Edition. Vol. 67.
[39] Tawarmalani, M. and N. V. Sahinidis, "A polyhedral branch-and-cut approach to global optimization", *Mathematical Programming*, 103(2), 225-249, 2005

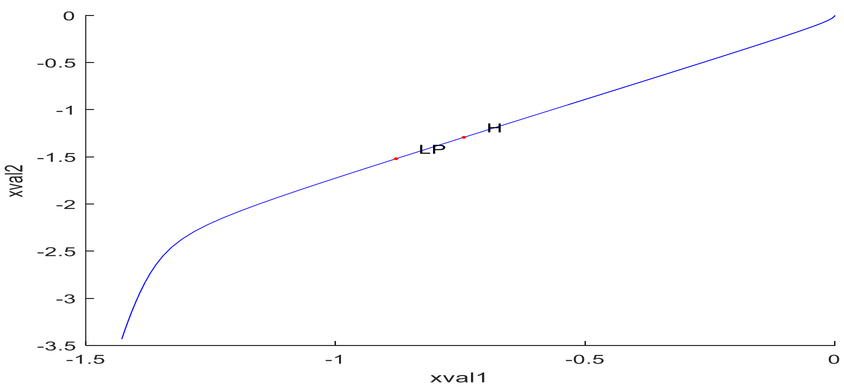

Fig. 1 Hopf Bifurcation and limit point without tanh activation factor

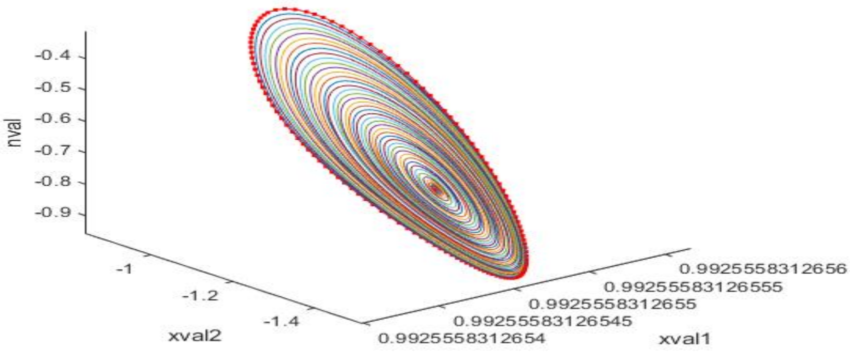

Fig. 2 Limit Cycle as a result of the Hopf Bifurcation point

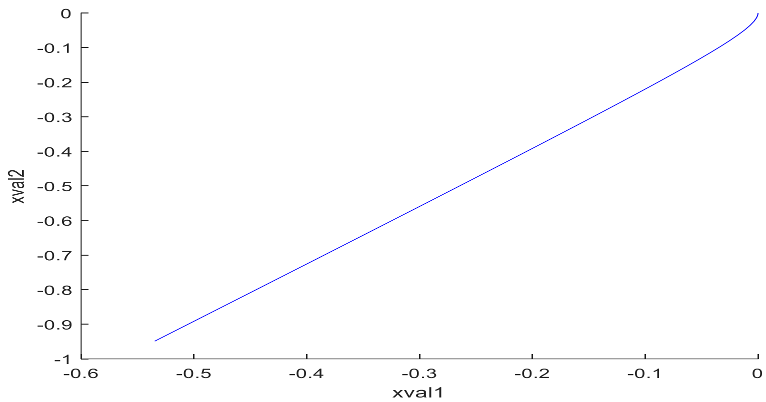

Fig. 3 Fig. 1 Hopf Bifurcation and limit point disappears with tanh activation factor

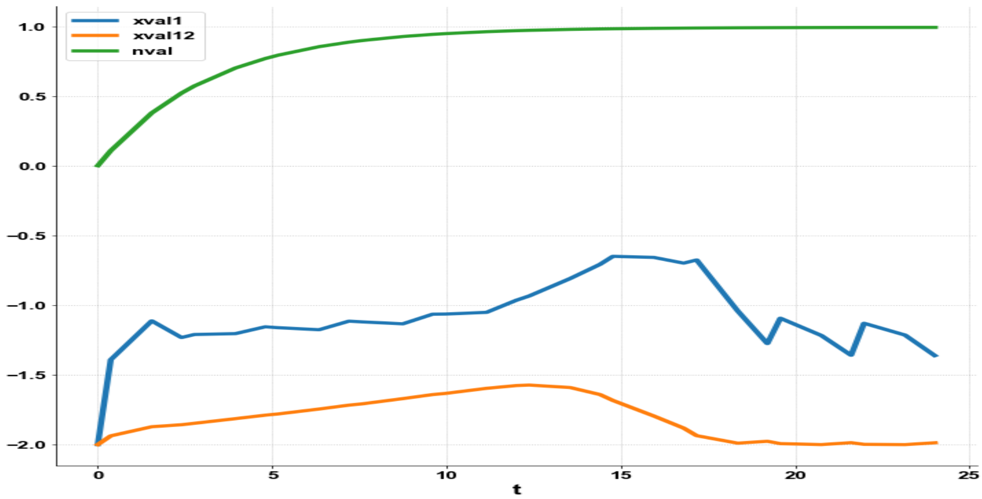

Fig. 4 xval1 xval2 and nval profiles without activation factor

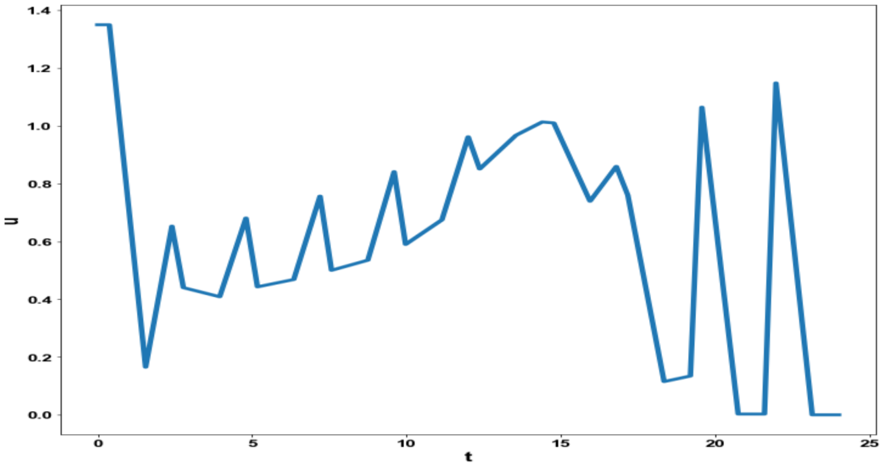

Fig. 5 u (control value) profile without activation factor

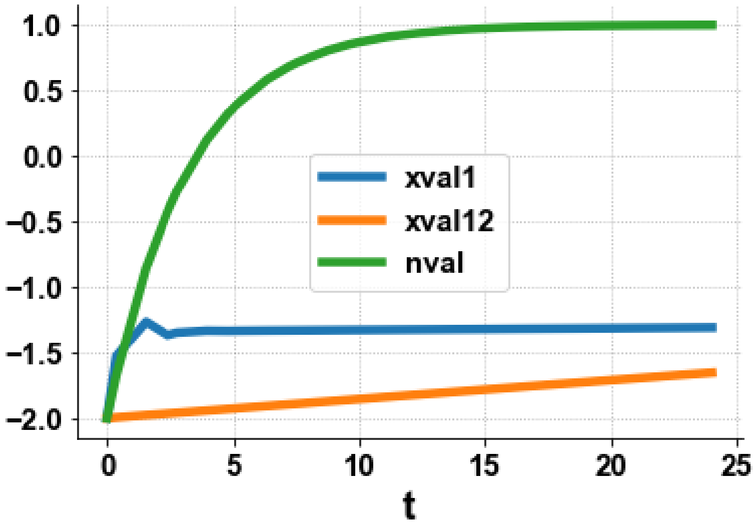

Fig. 6 xval1 xval2 and nval profiles with tanh activation factor

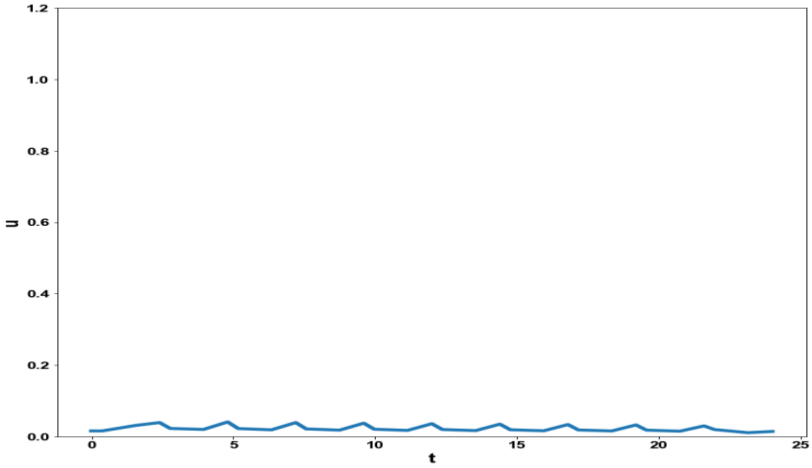

Fig. 7   u (control value) profile without activation factor